Growth of Non-Polar *a*-Plane AlGaN Epilayer with High Crystalline Quality and Smooth Surface Morphology

Abbas Nasir, Xiong Zhang, Sohail Ahmad, Yiping Cui

***Abstract*—**Non-polar a-plane AlGaN epilayers of high structural quality have been grown on *r*-sapphire substrate by using metalorganic chemical vapor deposition (MOCVD). A graded non-polar AlGaN buffer layer with variable aluminium concentration was used to improve the structural quality of the non-polar *a*-plane AlGaN epilayer. The characterisations were carried out by high-resolution X-ray diffraction (HR-XRD), atomic force microscopy (AFM) and Hall effect measurement. The XRD and AFM results demonstrate that the Al-composition-graded non-polar AlGaN buffer layer significantly improved the crystalline quality and the surface morphology of the top layer. A low root mean square roughness 1.52 nm is obtained from AFM, and relatively low background carrier concentration down to 3.9×10^{17} cm^{-3} is obtained from Hall effect measurement.

***Keywords*—**Non-polar AlGaN epilayer, Al composition-graded AlGaN layer, root mean square, background carrier concentration.

I. Introduction

In the past decade, AlGaN-based semiconductors have attracted much attention because of their potential applications in laser diodes, visible or ultraviolet (UV) light-emitting diode (LEDs), and high power transistors [1], [2]. In particular, the AlGaN-based UV-LED's operating in the deep UV spectral region have a wide range of potential applications such as disinfection of medical tools [3], water purification [4], as well as medical diagnostics and Phototherapy [5].

To date, most of the AlGaN-based UV-LEDs are generally fabricated with polar (0001)-oriented *c*-plane. Therefore, this is relatively easy to grow high crystalline quality polar AlGaN epilayers along *c*-direction [6]. However, the efficiency of the AlGaN-based UV-LEDs fabricated with the polar *c*-plane AlGaN materials can be reduced due to strong quantum-confined Stark effect induced by spontaneous and piezoelectric polarization electric field along the *c*-direction. Thus, non-polar *a*-plane AlGaN epilayers were considered to be the alternative materials for the fabrication of AlGaN-based UV-LEDs [7], [8].

Although, the epitaxial growth of non-polar *a*-plane AlGaN-based epilayers on semipolar *r*-plane sapphire substrate with either MOCVD or molecular beam epitaxy (MBE) has been a very challenging task. In fact, high dense superficial pyramidal defects have been usually observed on the surface of the non-polar *a*-plane AlGaN epi-layers, this is due to the strong anisotropy in growth rate along with various in-plane directions [9].

Although non-polar *a*-plane AlGaN is considered to be one of the most permeasible materials to fabricate the non-polar *a*-plane AlGaN-based UV-LEDs with much higher efficiency than that of the conventional polar AlGaN-based UV-LEDs [3]; but, there are still many problems to be solved with the non-polar *a*-plane AlGaN-based materials, such as poor crystalline quality and rough surface morphology, because the hetero-epitaxial growth of the non-polar *a*-plane AlGaN thin film on either sapphire or SiC substrate usually results in high densities of threading dislocations and stacking faults [10].

Various kinds of growth technologies were developed to improve the crystalline quality and surface morphology of the non-polar *a*-plane AlGaN epi-layers. Recently, the Al-composition graded layer method was reported to be more effective than conventional methods [10].

In this paper, the successful growth of the non-polar *a*-plane AlGaN epilayer with high crystalline quality and smooth surface morphology is reported. In particular, the impact of the application of the non-polar *a*-plane AlGaN layer on the optical and structural properties of the un-doped non-polar *a*-plane AlGaN layer has been studied in detail with HR-XRD and AFM. The characterization results show that the surface morphology and crystalline quality of the un-doped non-polar *a*-plane AlGaN epi-layers improved significantly with the introduction of the Al-composition graded non-polar *a*-plane AlGaN buffer layer.

II. Experimental

The epitaxial growth of the non-polar *a*-plane AlGaN epilayer samples were on 2-inch *r*-plane sapphire substrates in MOCVD reactor were performed. All the samples were grown in low pressure (40 Torr) in this work. Trimethyl-gallium (TMGa), trimethyl-aluminium (TMAl), and ammonia (NH_3) were used as the precursors for Ga, Al, and N, respectively, and hydrogen (H_2) was used as the carrier gas as described in detail in our previously published articles [11], [12]. Prior to the growth, the *r*-plane sapphire substrate was heated up to 1,080 °C for 5 minutes to remove the surface contamination. The sapphire substrate was kept at 1,080 °C in NH_3 and H_2 ambience for two minutes to perform the nitridation treatment. Then a 200 nm-thick non-polar high temperatures (HT) AlN

Abbas Nasir, Xiong Zhang, and Yiping Cui are with the School of Electronics Science and Engineering, Advanced Photonics Center, Southeast University, Nanjing 210096, Jiangsu China (e-mail: abbasnasir02@gmail.com, xzhang62@aliyun.com, cyp@seu.edu.cn).
Sohail Ahmad is with the Faculty of Material Science and Engineering, Kunming University of Science and Technology, Kunming, 650093, Yunnan, China (e-mail: Sohail.awkum@gmail.com).

buffer layer was deposited on the sapphire substrate at 1,130 °C to decrease the lattice mismatch. Afterwards, the Al composition-graded non-polar AlGaN layer with the Al composition varied from 1 to 0.45 was deposited on the non-polar HT-AlN buffer layer. Finally, the non-polar *a*-plane AlGaN epilayer with constant Al composition but with varied layer thicknesses was grown on the non-polar Al composition-graded AlGaN layer to check the surface morphology and crystalline quality.

All three samples, S_1-S_3, were cut into square pieces with the size of 1×1 cm^2. HR-XRD and AFM were used to evaluate surface roughness and crystalline quality. The Al composition was determined based on the XRD and UV-visible absorption spectrum (not shown here). The Hall effect measurements were conducted at room temperature by using the van der Pauw method and indium as the Ohmic contact with an Ecopia Hall measurement system under a magnetic field of 0.35 T. The schematic layer structure for the non-polar *a*-plane AlGaN epilayer samples with varied layer thickness is shown in Fig. 1.

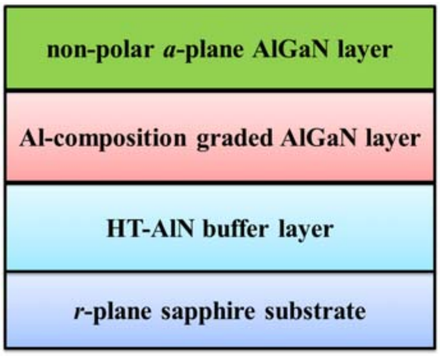

Fig. 1 Schematic layer diagram of non-polar *a*-plane AlGaN with Al-composition-graded-AlGaN layer

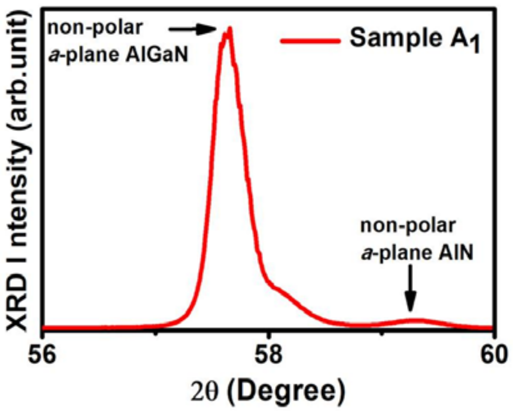

Fig. 2 HR-XRD 2θ-ω scanning curve for *a*-plane AlGaN sample S_1

III. Results and Discussion

Three samples were designed named as samples S_1-S_3 of the non-polar *a*-plane AlGaN epi-layers. These samples were grown with the same structure except the last AlGaN layer thickness increase, with the increase of thickness for each sample which shows a significant effect on the surface and crystalline quality of the samples S_1-S_3. The attained result shows by HR-XRD and AFM technique.

Fig. 2 shows the HR-XRD 2θ-ω curve of sample S_1. The different peak values located at $2\theta = 57.67^o$ and 59.39° respectively which verify the $[11\bar{2}0]$ −oriented non-polar *a*-plane AlGaN and non-polar AlN [13]-[15]. The curves of 2θ-ω for all the samples S_2 and S_3 are very similar as of sample S_1 not shown in Fig. 1.

The Al composition for the entire samples S_1-S_3 was determined 0.29 by HR-XRD and confirmed with UV-spectroscopy (not shown here) at room temperature. Moreover, the full width at half maximum (FWHM) results of non-polar *a*-plane AlGaN epilayers XRs curves of samples S_1-S_3 grown with increasing of thickness with constant increasing of thickness from 120 to 310 nm respectively are shown in Fig. 3, which are measured and summarized in Table I. It can be seen that the values of S_2 are smaller than the value of S_1 which shows a great effect of non-polar *a*-plane AlGaN thickness on Al composition-graded AlGaN buffer layer. These phenomena can be explained in terms of that with increasing of thickness of non-polar *a*-plane AlGaN layer on Al-composition-graded AlGaN buffer layer underwrite to the climb or slip of the residual strain dislocation, simplifies interaction and extinction of defects. Thus in results, the crystalline quality improved [7], [16], [17]. But still, with the increasing of non-polar *a*-plane AlGaN layer thickness on Al-composition-graded AlGaN layer the defect density and lattice distortion could also be increased, this could be because the growth of the non-polar *a*-plane AlGaN epilayer is larger than the atomic size of Ga or Al atom, persuading the degradation in the crystalline quality. In the meantime, with the increase of thickness of non-polar *a*-plane AlGaN layer, which is might also be responsible for the degradation in the crystalline quality. As a result, an increase in FWHM shown in Table I with further increasing of thickness of non-polar *a*-plane AlGaN layer. On the other hand, we characterized all samples S_1-S_3 by AFM to study their morphological properties. On first sample, we observe a modulation of the surface topography at a larger scale on the surface of the sample as shown in Fig. 4, as well the surface morphology is also very rough as shown in Table I. But in the second sample, the surface morphology decreased as the non-polar *a*-plane AlGaN layer thickness has an increase from 120 to 205 nm respectively to 1.56 nm from 18.8 nm. Moreover, As further increasing of thickness with with the same Al composition and structure the RMS value increased again to 4.96 nm within the surface area of 5×5 μm^2 [18]. The sample S_2 surface morphology is 95% less than as compared with the sample S_1 showing the smoothest surface as compared to the other samples S_1 and S_3, which can be seen in three-dimensional images (3D) of AFM, Fig. 3. Usually, the enhancement in surface morphology can be attributed in the development in surface morphology as well the reduction of the residual strain of non-polar *a*-plane AlGaN epilayers [19]. As we increase the thickness of the non-polar *a*-plane AlGaN layer the RMS value increases again. However, the surface roughness of sample S_3 increases again as compared to sample

S_1 which can be explained in terms of theory that the growth mode transform from 2D (dimension) to 3D when the thickness of the non-polar *a*-plane AlGaN epilayers increases [20]. This shows that with the increase of growth time for AlGaN layer is very effective on graded layer.

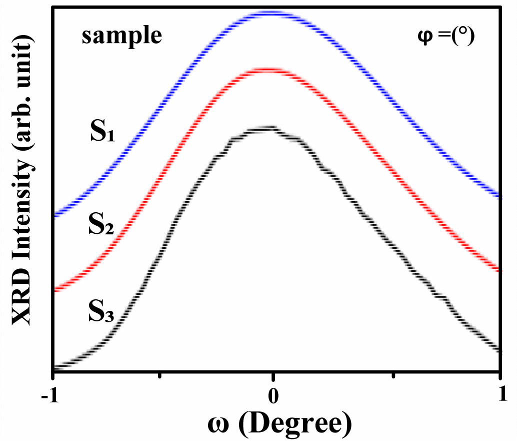

Fig. 3 XRC curves for all samples S_1-S_3 of non-polar *a*-plane AlGaN measured along [0001] direction

TABLE I
SUMMARY OF VARIED THICKNESS OF NON-POLAR *A*-PLANE ALGAN LAYER ON AL-COMPOSITION-GRADED ALGAN LAYER, XRC FWHM RESULTS FOR ALL SAMPLES S_1-S_3 BESIDE [0001] AT Φ=(°) AND RMS RESULTS

Sample	S_1	S_2	S_3
Thickness of the non-polar *a*-plane AlGaN layer (nm)	120	205	310
FWHM(arc sec) (°)	1101	663	964
RMS Value (nm)	18.8	1.52	4.92

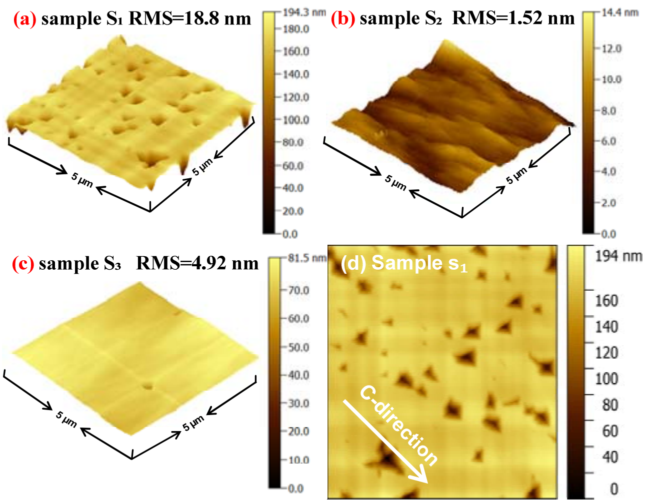

Fig. 4 AFM images of non-polar *a*-plane AlGaN epilayers samples S_1-S_3 shows with area 5×5μm^2

The background electron concentration of the non-polar *a*-plane AlGaN decreases to -3.9×10^{17} cm^{-3} with the varied thickness of the non-polar *a*-plane AlGaN layer. Similarly, for all the samples from S_1-S_3 as a function of thickness of non-polar *a*-plane AlGaN epilayers are obtained from Hall Effect measurement at room temperature. On the other hand, the native background electron concentration decreases from -10^{18} to -3.9×10^{17}cm^{-3} unintentionally. It is well accepted that to achieved unintentional high background electron concentration because of the oxygen impurities which act as a donor to the GaN epilayers. Although first principle shows that oxygen will undergo a DX transition in $Al_xGa_{1-x}N$ when x > 0.3 which will behave like a big acceptor [21]. That's why oxygen impurities not responsible for the high background electron concentration. The decrease in background electron concentration can be attributed to the decrease in the V_N density. Same conclusion was also found that the decrease in native electron concentration is due to V_N is the native major source of the carrier in GaN epilayers [22].

IV. CONCLUSIONS

In this work, non-polar *a*-plane AlGaN epilayer with the increasing of thickness on Al composition-graded AlGaN buffer layer can be grown with high temperature, having droplet free surface morphology were studied. Therefore, the RMS value as small as 1.52 nm found from the AFM measurement, as well RT-PL was also succeeded with the same sample. On the other hand, back ground electron concentration (BEC) as low as -3.9550×10^{17} cm^{-3} was achieved. These results show that the defects and misfit dislocations of non-polar *a*-plane AlGaN epi-layers could be significantly reduced with the increasing of non-polar *a*-plane AlGaN epi-layers thickness on Al composition-graded non-polar *a*-plane AlGaN layer. The improvement in both the surface morphology and crystalline quality for the non-polar *a*-plane AlGaN epi-layers achieved in this study can cover the way to fabricate non-polar AlGaN based LEDs.

ACKNOWLEDGMENT

This work was supported by National Key Research and Development Program of China (Grant No. 2018YFE0201000), the Fundamental Research Funds for the Central Universities, Postgraduate Research & Practice Innovation Program of Jiangsu Province (Grant No. KYCX18_0071) and National Natural Science Foundation of China (61804027), Natural Science Foundation of Jiangsu Province (BK20180359).

REFERENCES

[1] Cho, C.-Y., et al., *Enhanced emission efficiency of GaN-based flip-chip light-emitting diodes by surface plasmons in silver disks.* Applied Physics Express, 2012. 5(12): p. 122103.
[2] Shur, M.S. and R. Gaska, *Deep-ultraviolet light-emitting diodes.* IEEE Transactions on electron devices, 2009. 57(1): p. 12-25.
[3] Würtele, M., et al., *Application of GaN-based ultraviolet-C light emitting diodes–UV LEDs–for water disinfection.* Water research, 2011. 45(3): p. 1481-1489.
[4] Chen, R.Z., S.A. Craik, and J.R. Bolton, *Comparison of the action spectra and relative DNA absorbance spectra of microorganisms: Information important for the determination of germicidal fluence (UV dose) in an ultraviolet disinfection of water.* Water research, 2009. 43(20): p. 5087-5096.
[5] Meduri, N.B., et al., *Phototherapy in the management of atopic dermatitis: a systematic review.* Photodermatology, photoimmunology & photomedicine, 2007. 23(4): p. 106-112.

[6] He, J., et al., *Study of NH3 flow duty-ratio in pulsed-flow epitaxial growth of non-polar a-plane Al0. 34Ga0. 66N films.* Materials Science in Semiconductor Processing, 2019. 90: p. 219-224.
[7] Laskar, MR, et al., *High-resolution X-ray diffraction investigations of the microstructure of MOVPE grown a-plane AlGaN epilayers.* Journal of Crystal Growth, 2011. 315(1): p. 208-210.
[8] Jo, M., et al., *Structural and electrical properties of semipolar (11-22) AlGaN grown on m-plane (1-100) sapphire substrates.* physica status solidi c, 2017. 14(8): p. 1600248.
[9] Waltereit, P., et al., *Nitride semiconductors free of electrostatic fields for efficient white light-emitting diodes.* Nature, 2000. 406(6798): p. 865-868.
[10] Nasir, A., et al., *Effects of indium surfactant and MgN intermediate layers on surface morphology and crystalline quality of non-polar a-plane AlGaN epi-layers.* Optik, 2019: p. 162978.
[11] Fan, A., et al., *Enhanced hole concentration and improved surface morphology for non-polar a-plane p-type AlGaN/GaN superlattices grown with indium-surfactant.* Superlattices and Microstructures, 2019. 130: p. 396-400.
[12] Wu, Z., et al., *Enhanced structural and electrical properties of non-polar a-plane p-type AlGaN/GaN superlattices.* Superlattices and Microstructures, 2019. 125: p. 310-314.
[13] Yang, H., et al., *γ-Aminobutyric acid ameliorates fluoride-induced hypothyroidism in male Kunming mice.* Life sciences, 2016. 146: p. 1-7.
[14] Dai, Q., et al., *Effects of Mg-doping on characteristics of semipolar (112¯2) plane p-AlGaN films.* Materials Letters, 2017. 209: p. 472-475.
[15] Laskar, MR, et al., *Distorted wurtzite unit cells: Determination of lattice parameters of non-polar a-plane AlGaN and estimation of solid phase Al content.* Journal of Applied Physics, 2011. 109(1): p. 013107.
[16] Yu, HB, et al., *Advantages of AlGaN-based deep-ultraviolet light-emitting diodes with an Al-composition graded quantum barrier.* Optics Express, 2019. 27(20): p. A1544-A1553.
[17] Hiroki, M. and K. Kumakura, *Ohmic contact to AlN:Si using graded AlGaN contact layer.* Applied Physics Letters, 2019. 115(19): p. 4.
[18] Zhao, J., et al., *Defects reduction in a-plane AlGaN epi-layers grown on r-plane sapphire substrates by metal organic chemical vapor deposition.* Applied Physics Express, 2016. 10(1): p. 011002.
[19] Tao, P., et al., *Crack-free Al0. 5Ga0. 5N epilayer grown on SiC substrate by in situ SiNx interlayer.* Materials Science in Semiconductor Processing, 2016. 41: p. 291-296.
[20] Tang, K., et al., *The roles of buffer layer thickness on the properties of the ZnO epitaxial films.* Applied Surface Science, 2016. 388: p. 557-564.
[21] Van de Walle, C.G., *DX-center formation in wurtzite and zinc-blende Al x Ga 1− x N.* Physical Review B, 1998. 57(4): p. R2033.
[22] Zhang, G., et al., *Relationship of background carrier concentration and defects in GaN grown by metalorganic vapor phase epitaxy.* Applied physics letters, 1997. 71(23): p. 3376-3378.